

**CATALYTIC REFORMING OF C5 TO C12 NAPHTHA
MODELED THROUGH THE KINETIC MODELING TOOLKIT**

by

Carl Burgazli

A thesis submitted to the Faculty of the University of Delaware in partial fulfillment of the requirements for the degree of Honors Bachelor of Chemical Engineering with Distinction

Spring 2013

© 2013 Carl Burgazli
All Rights Reserved

**CATALYTIC REFORMING OF C5 TO C12 NAPHTHA
MODELED THROUGH THE KINETIC MODELING TOOLKIT**

by

Carl Burgazli

Approved: _____
Michael T. Klein, Ph.D.
Professor in charge of thesis on behalf of the Advisory Committee

Approved: _____
Prasad Dhurjati, Ph.D.
Committee member from the Department of Chemical Engineering

Approved: _____
Susan Groh, Ph.D.
Committee member from the Board of Senior Thesis Readers

Approved: _____
Michael Arnold, Ph.D.
Director, University Honors Program

ACKNOWLEDGMENTS

I would like to thank my family for their patience with me and my procrastinating nature throughout my entire academic career, along with Dr. Michael T. Klein and the entire Klein research group for the opportunity to develop with and learn about complex computational kinetics.

TABLE OF CONTENTS

LIST OF TABLES	vi
LIST OF FIGURES	vii
ABSTRACT	viii
1 INTRODUCTION	1
1.1 Modeling Motivation	1
1.2 Modeling Methods	2
1.2.1 Lumped Modeling	2
1.2.2 Mechanistic Modeling	3
1.2.3 Reaction Pathways Modeling	4
1.3 The Kinetic Modeling Toolkit	5
1.3.1 The Interactive Network Generator	6
1.3.2 The Composition Modeling Editor	7
1.3.3 The Kinetic Modeling Editor	8
2 THE CATALYTIC REFORMING MODEL	10
2.1 Kinetic Model Principles	10
2.1.1 Langmuir-Hinshelwood Mechanism	10
2.1.2 Surface Adsorption Equilibrium Constant	11
2.1.3 Arrhenius Equation	11
2.1.4 Linear Free Energy Relationship	12
2.2 Reaction Families	13
2.2.1 Aromatization	13
2.2.2 Ring Formation	13
2.2.3 Isomerization	14
2.2.4 Paraffin Cracking	14
2.2.5 Ring Isomerization	15
2.2.6 Side Chain Cracking	15
2.2.7 Dealkylation	15

3	EXPERIMENTAL SETUP	16
3.1	System Apparatus	16
3.2	Experimental Data and Data Processing	16
3.3	Initial Estimates	18
3.4	Tuning Method	19
3.5	Individual Reactions	21
3.6	Carbon Length Dependence	21
4	RESULTS	23
4.1	Overall Parity Plot	23
4.2	Aromatic Analysis	24
4.3	Isoparaffin Analysis.....	25
4.4	Paraffin Analysis	26
4.5	Naphthene Analysis.....	27
5	FUTURE WORK	28
5.1	Temperature Dependence	28
5.2	Semi-Regenerative Reforming	29
5.3	Overall Refinery Model.....	30
6	CONCLUSIONS	31
	REFERENCES	32
	ADDITIONAL FIGURES AND TABLES	34

LIST OF TABLES

Table 1:	Number of Reactions Necessary for Different Modeling Schemes	5
Table 2:	Summary of Initial Tuning Estimates	19
Table 3:	Catalytic Reforming Model Output Totals from INGen	34
Table 4:	PIANO Summary of Effluent From Catalytic Reformer	34
Table 5:	Raw Tuned Parameters of Reforming Model.....	35

LIST OF FIGURES

Figure 1:	CME Output for the Reforming Model, as seen by KME.....	8
Figure 2:	Simplified Reaction Families in KME	9
Figure 3:	Species Input Sheet from KME.....	18
Figure 4:	KME Tuning Sheet, with Some Reaction Parameters Activated.....	20
Figure 5:	Overall Parity Plot of the Catalytic Reforming Model.....	23
Figure 6:	Aromatic Parity of the Catalytic Reforming Model	24
Figure 7:	Isoparaffin Parity of the Catalytic Reforming Model	25
Figure 8:	Paraffin Parity of the Catalytic Reforming Model	26
Figure 9:	Aromatic Parity Plots for Varying Temperatures.....	28
Figure 10:	Simplified Flowsheet of Semi-Regenerative Reforming	29
Figure 11:	Raw Reaction Equations of Catalytic Reforming Model in KME.....	36
Figure 12:	Reaction Constants of Catalytic Reforming Model in KME	36
Figure 13:	Overall Parity Plot, Prior to Inclusion of A7 Individual Reaction	37

ABSTRACT

Modeling the behavior of the catalytic reforming process requires complex kinetics and computational rigor to give accurate results. Using 15 different reaction groups in a pathways-level model applied to the Kinetic Modeling Toolkit (KMT), a predictive model is generated to account for the network of reactions experienced in a catalytic reformer. The accuracy of the overall model fits the linear regression: $y_{i,\text{calculated}} = 0.9447 y_{i,\text{observed}}$ with an R^2 value of 0.7628. The accuracy of the aromatic fit is far higher ($R^2 = 0.8088$) while the isomerization reactions have little predictive relation between observed and calculated species. In accounting for the temperature dependence of the reactions, the model would be able to predict the behavior of semi-regenerative reformers and overall refinery modeling overall.

Chapter 1

INTRODUCTION

1.1 Modeling Motivation

The need for a strong computational kinetic model for catalytic reforming stems from the process and feedstock itself. Upon arrival at the refinery, crude oil is first distilled to separate the heavier and lighter components (usually indicated by the number of carbons, or their C#, for convenience). One tray, the C5 through C12 cut, constitutes a significant portion of the feedstock and is of such a carbon length that it is applicable for use in an internal combustion engine¹.

This feed, however, is not quite ready for general consumer consumption. This feed is not a desirable product for the engine, as at this point the C5-C12 feed has a very low octane rating due to its composition of largely normal paraffins. In order for this material to have substantial benefit as a fuel (and prevent unnecessary engine knock), the feed must be reformed to produce a larger proportion of isoparaffins and aromatics in the product. This is achieved through the use of a catalytic reformer, transforming the feed from a low octane, undesirable product to a high octane product nearly complete for sale. To achieve the final product, a zeolite catalyst (most frequently a platinum-alumina hybrid) is used to speed up the process and increase selectivity for aromatics, which are the most desirable.

The catalytic reforming process, however, is highly complex. This is due primarily to the complexity of the C5-C12 feedstock. In this feed, there are hundreds of different reactants that could undergo thousands of different reactions within the

catalytic reactor. Due to this complexity, it is necessary to develop a strong computational model to characterize the model and to show how temperature, pressure, and compositional changes to the process will alter the final product (critical for maximizing octane improvement). Therefore, in order to produce high octane product through the catalytic reformer, a computational-intensive model must be created.

1.2 Modeling Methods

The processed petroleum industry, being a century old, already has multiple attempts at capturing the kinetic behavior of the C5-C12 feed in the catalytic reformer. These modeling methods can be sorted three categories: lumped models, mechanistic models, and pathways models².

1.2.1 Lumped Modeling

The simplest applicable modeling method applicable for catalytic reforming is that for a lumped model. A lumped model is one that groups together reacting species by a physical property (most frequently boiling point) as one reacting species, each with its own reaction formula. This method is useful when physical property data is scarce (only one physical property, the one the lumps are being designed for, is used) and limited computational power is available.

Lumped models, however, have significant limitations. Since the models rely on the assumption that all species within each lump have a similar reaction behavior (when instead they are determined by physical properties), it is assumed that all species having the shared physical property all have similar kinetics. This underscores the possibility of some species of the lump having slower side reactions that, although

they are not experienced by the lump as a whole, change the concentrations of species in other lumps. Since the concentration of these species within the lumps are not accounted for by the lump as a whole, changes in their relative concentrations to the lump as a whole is unpredictable, and so the effects of these side reactions are not accounted for by the model, adding significant variability. Furthermore, the general effect of species in one lump on another lump (such as one particular isomer in a naphthene lump undergoing an aromatization reaction to one particular isomer in an aromatic lump) is not capable of being predicted by a lumped model. Therefore, the lumped model's inherent inability to predict strong changes in concentration to species within the lumps, along with the inability for lumps to predict varying effects of side reactions, indicates that a lumped model is an undesirable model design when stronger computational power is available.

1.2.2 Mechanistic Modeling

A far more complex modeling method that can be employed on catalytic reforming is that of the mechanistic model. The mechanistic model derives the behavior for every possible species in the reaction feed from first principles. Due to this, a mechanistic model is capable completely predicting the kinetic behavior of any feed that is given to the catalytic reformer, as well as the behavior that it would predict on any given zeolite. Therefore, a mechanistic model addresses the lack of flexibility and accuracy present in a similarly applied lumped model.

Mechanism-based modeling, though, also has significant drawbacks. While it is more predictive than a lumped model, the resources required for a mechanistic model to work (in the form of both CPU time and feed composition data) are enormous. Every possible reaction and reactant has to be accounted for, regardless of

initial concentration in the reaction (due to reverse reactions). All of the reaction steps for each reaction (which each has its own reaction rate and concentration basis) must also be accounted for, which is beyond the capability of modern computing. The magnitude of the number of reactions needed by a mechanistic model relative to other models is outlined in Table 1³. Furthermore, reaction intermediates, although only present in extremely small quantities for a short period of time, are needed for determining reaction rates. These reaction intermediates are nearly impossible to measure due to their small concentrations and have large errors on their measurements, adding significant variability to an otherwise exact model. This results in very stiff ordinary differential equations, which are inherently difficult to solve. Therefore, because the inherent complexity cannot be accurately quantified nor effectively managed in a reasonable timescale by modern computational methods, a mechanistic model is unfeasible for a catalytic reforming model.

1.2.3 Reaction Pathways Modeling

In terms of complexity, the reaction pathways (or simply “pathways”) model takes a middle ground between lumped and mechanistic models. Pathways modeling, like lumped modeling, is based upon an a priori solution of the reaction mechanism, realized in the form of the rate law using lumped parameters (types of reactions reactions). A pathways model differentiates itself from a lumped modeling scheme in that it keeps track of the molecules present in the reacting mixture. This focus on reaction groupings (or families) means that all major species that are part of each type of reaction have to be measured, increasing the number of reactants that have to be accurately measured. However, every reaction that is part of the reaction family has a similar reaction design and rate, removing the necessity of measuring reaction

intermediates (as indicated in Table 1). Furthermore, the computational power needed to fit a pathways model to existing data is within reach of modern computing.

Therefore, a reaction pathways model is suitable for the complexity that is inherent in the catalytic reforming process.

The use of pathways modeling schemes has been employed previously in industry by the large oil corporations, most notably in the models of Mobil[®] with KinPTR⁴ and Exxon[®] with POWERFORMING⁵. The Exxon and Mobil models, in addition to modeling the feed by reactant type (paraffin, isoparaffin, naphthene, aromatic) had lumped the reaction kinetics by carbon number. These models, although accurate, were limited in complexity by the computational resources utilized in their construction. This motivates the use of the pathways modeling method on a more computationally rigorous model.

Table 1: Number of Reactions Necessary for Different Modeling Schemes

Cumulative Carbon Number	Number of Reacting Species	
	Mechanistic	Pathways
5	40	10
6	81	18
7	148	33
8	358	69
9	654	152

1.3 The Kinetic Modeling Toolkit

To develop the complex pathways kinetic model that is necessary to accurately describe the catalytic reforming model, a computational model generator must be employed. Attempting to keep track of the hundreds of reacting species necessary for the reforming model and generate the reactions manually would add a lengthy step to

the model creation process as well as introduce human error in deciding the importance of chosen reactions. To generate the complete catalytic model, the Kinetic Modeling Toolkit (KMT) developed by Dr. Michael T. Klein's research group is used. This toolkit comprises three independent tools which generate any complex organic model from the ground up: the Interactive Network Generator (INGen), the Composition Modeling Editor (CME), and the Kinetic Modeling Editor (KME).

1.3.1 The Interactive Network Generator

To develop any model, a list of reactions and species considered the basis of the model must be sorted. It is only after the species and all the relevant and related reactions of the model are compiled (a reaction network) that the model can be constructed. This reaction network generation is done using KMT's Interactive Network Generator (INGen). To develop a network of related and relevant reactions, INGen first uses a list of reactants and reactions the modeler has deemed most important for the model (a model "seed") to generate the base model. INGen then follows the reaction path (the products from one reaction being the reactants of another reaction, the products of that following reaction being the reactants yet another reaction, etc.) for a length as defined by the user (its "rank"), finding any overlap between the many reaction paths to determine which reactions and newly introduced species are truly relevant. Finally, these relevant reactions are organized into the user defined reaction families to create the basis for the model.

INGen generates the basis for the catalytic reforming model by first taking the major species for each carbon number (C5 through C12) and for each group of hydrocarbon (paraffin, isoparaffin, naphthene, and aromatic). This seed then determines the important reactions through a rank of two. Finally, all of the reactions

are sorted into the 14 previously determined reaction families to create the reaction basis of the pathways model, which is presented in Table 3 in the Appendix.

1.3.2 The Composition Modeling Editor

With the completion of the reaction network, reaction rate constants can be applied to each reaction network to match the model to experimental data. However, without physical properties of the species in the reaction (in particular, the enthalpy of formation), the minor differences in the reactions present in each reaction family due to physical species cannot be accounted for. This inability to account for the small differences in a lump is the factor that most inhibited the lumped modeling method, and therefore must be addressed. To bring in these physical properties of the species in the reaction network, the Composition Modeling Editor (CME) tool is used. CME approximates the physical properties from literature data and models, which is then verified by experimental data. The physical properties are used to address physical differences in the reacting species in each reaction pathway. The physical properties for the catalytic reforming model are sent to the Kinetic Modeling Editor (shown in Figure 1) and are applied to the reforming kinetic model, as described in Chapter 2.

B	C	D	E	F	G	H	I
SCode	Tref(K)	Tc(K)	Pc(K)	Vc(K)	Tb(K)	Tm(K)	Hform(Kcal/mol)
RF1	298	0	0	0	0	0	0
RF2	298	0	0	0	0	0	0
RF3	298	0	0	0	0	0	0
RF4	298	0	0	0	0	0	0
RF5	298	0	0	0	0	0	0
RF6	298	0	0	0	0	0	0
RF7	298	0	0	0	0	0	0
RF8	298	0	0	0	0	0	0
RF9	298	0	0	0	0	0	0
RF10	298	0	0	0	0	0	0
RF11	298	0	0	0	0	0	0
RF12	298	0	0	0	0	0	0
RF13	298	0	0	0	0	0	0
RF14	298	0	0	0	0	0	0
species1	298	560.483748	41.286499	303.39	355.500492	181.284629	-25.33516746
species23	298	661.688562	22.769627	600.19	482.72552	216.50261	-55.56076555
species24	298	663.256773	23.378005	584.62	480.802245	221.903947	-54.90885167
species33	298	592.842233	30.365855	437.09	396.469427	183.535556	-40.60598086
species46	298	643.358559	24.800614	543.91	463.780971	207.704376	-50.5777512
species47	298	645.055665	25.523823	528.34	461.685995	213.431446	-49.92583732
species53	298	623.449493	27.22378	487.63	443.072386	198.347656	-45.59473684
species54	298	621.045428	28.422735	481.2	427.847633	191.443828	-46.98971292
species62	298	650.197223	25.395405	533.34	469.650938	215.606752	-47.92535885

Figure 1: CME Output for the Reforming Model, as seen by KME

1.3.3 The Kinetic Modeling Editor

To calculate the outcome of a computational model, which then can be compared to experimental data for accuracy, the Kinetic Modeling Editor (KME) is used. KME can either utilize user-designed reactions to build a model (as shown in Figure 2) or import an entire reaction network generated by INGen and build the model to match the reaction families that have been previously specified (Figures 11 and 12 in the Appendix). Using this built model, along with the physical property data imported from CME, the model's reaction constants can be fitted to experimental data and process equipment using optimization algorithms (otherwise known as “tuning.”) Following this, the tuned model can then be used to predict products from differing reactant feeds and reactor designs.

C:\KME5.0\Models\A-B-C-SAM\rate.eqn		RELOAD	S
REACTIONS		RATE LAW	
1	[L] + A <=> B + [L]	rxn[0] = k(lgA1,E1)*(y[A]*y[L] - y[B]*y[L]/Keq[0]);	
2	[L] + B <=> C + [L]	rxn[1] = k(lgA2,E2)*(y[L]*y[B] - y[C]*y[L]/Keq[1]);	
3	#SAM		
4	C + [L] -> C[L]		
5			
6			
7			
8			
9			
10			
11			
12			
13			
14			

Figure 2: Simplified Reaction Families in KME

For the catalytic reforming model, the complex reaction network must be imported from INGen and have the various physical property data retrieved from CME. The model is then built using the KME generation tools, examples of which are displayed in Figures 11 and 12 in the appendix. This model is formulated using the principles outlined in Chapter 2.

Chapter 2

THE CATALYTIC REFORMING MODEL

2.1 Kinetic Model Principles

To develop a pathways model that is not only capable of accounting for the variance present in the reactions within a reaction family but also presenting clear reaction constants on which the catalytic reforming model can be tuned, a similar reaction form must be applied to all reaction families. In doing so, and applying simplifications, tunable constants can be isolated and adjusted by the computer.

2.1.1 Langmuir-Hinshelwood Mechanism

In catalytic reforming, it is assumed that the reactions occurring on the surface of the catalyst are occurring far more quickly than those in the bulk fluid⁶. Therefore, the kinetic model can be isolated to only concerning itself with surface kinetics, which is expressed through the Langmuir-Hinshelwood mechanism to be

$$r_i = k_i \times \frac{K_{eq,i} \left(y_i - \frac{y_i^P}{K} \right) y_{cat}}{\left(1 + \sum_{j=1}^n K_{eq,j} y_j \right)^n} \quad (1)$$

where r_i is the rate of the given reaction, k_i is the Arrhenius rate constant, $K_{eq,i}$ is the surface adsorption equilibrium constant, y_i is the concentration of the reactant, y_i^P is the concentration of the product, K is the reaction constant, and y_{cat} is the concentration of the catalyst in the reactor (in moles/liter). The denominator term of the mechanism accounts for the interaction of all the species and their adsorption onto the zeolite catalyst.

2.1.2 Surface Adsorption Equilibrium Constant

To determine the magnitude of the equilibrium constant for each species as it is adsorbed onto the zeolite catalyst (alumina, in the case of the catalytic reforming model), surface kinetics equations developed by Klein's research group⁷ were used. For the alumina catalyst in a catalytic reformer, all of the species bind to the acid sites of the catalyst. The equilibria of this behavior are defined as

$$\ln K_{eq,i} = 0.182 + \frac{1.93N_{AR} + 0.187N_{SC}}{RT} \quad (2)$$

Where N_{AR} and N_{SC} are the number of aromatic rings and saturated carbons of the adsorbing species, respectively, $K_{eq,i}$ is adsorption constant, R is the gas constant, and T is the temperature in Kelvin. N_{AR} and N_{SC} are both imported data from the analysis run through CME. None of these terms, however, are tunable parameters (all fixed and predefined), and therefore only serve to create another source accounting for reaction variance within the reaction families.

2.1.3 Arrhenius Equation

To address the effect of a reaction rate constant on the reaction rate, the simple yet accurate Arrhenius equation is used to evaluate the value of k_i :

$$\ln k_i = \ln A - \frac{E^*}{RT} \quad (3)$$

This form shows a tunable parameter of the model: the pre-exponential factor A . This term is used to indicate the collision frequency of the reaction, and therefore is the same across all members of a reaction family. The activation energy (E^*), however, is a term that is different for every reaction. Therefore, a method of differentiating the activation energy is needed.

2.1.4 Linear Free Energy Relationship

The uniqueness of the activation energy term in every reaction initially removes the capability of having a tunable model, since the activation energies of the individual reactions are not physical properties that can be predicted by CME.

However, upon rearranging the Arrhenius equation from thermodynamic principles:

$$\ln k_i = \ln A + \frac{\Delta S_{rxn}^*}{R} - \frac{\Delta H_{rxn}^*}{RT} \quad (4)$$

$$\ln \frac{k_j}{k_i} = \frac{\Delta(\Delta S_{rxn}^*)}{R} - \frac{\Delta(\Delta H_{rxn}^*)}{RT} \quad (5)$$

Where k_i and k_j are the reaction rate constants for two different reactions in the same reaction family. Being in the same reaction family, it is assumed that there are no significant steric differences between the molecules undergoing reaction in the two different molecules⁸. Due to this, $\Delta(\Delta S_{rxn}^*) = 0$. Furthermore, since $\Delta H_{rxn}^* = E_a + RT$:

$$\ln \frac{k_j}{k_i} = -\frac{\Delta(E_{a,j} + RT - E_{a,i} - RT)}{RT} = -\frac{\Delta E_a}{RT} \quad (6)$$

Finally, the linear free energy relationship developed by Polanyi⁹ is used, stating that

$$E_a = E_0 - \alpha \Delta H_{rxn} \quad (7)$$

where E_0 is an average activation energy for the entire reaction family, and alpha is a correction parameter that accounts for the differences between each reaction in the reaction family. E_0 and alpha, both being constants for the entire reaction family, are tunable. This results in

$$k_i = 10^{\log A} e^{\frac{(E_0 - \alpha \Delta H_{rxn})}{RT}} \quad (8)$$

where $\log(A)$, E_0 , and alpha are all tunable parameters in KME.

2.2 Reaction Families

Following the creation of the relevant reaction network by INGen, the reactions were sorted into 14 different reaction families that, due to the similarity in how the reactions behaved on the surface of the catalyst, fulfilled the requirements of the simplifications needed for the linear free energy relationships to hold. Because of this, these reaction families are capable of being tuned while also accurately reflecting similarity in chemistry that occurs on the catalyst.

2.2.1 Aromatization

The dehydrogenation of naphthenes, or aromatization, occurs when a cyclohexane ring within the compound stabilizes itself by forming a benzene ring, releasing three hydrogen molecules in the process. This process is both endothermic extremely fast (by over four orders of magnitude more than the next preceding reaction rate). Tracking this set of reactions is vital, since aromatics are desirable for their high octane content, but are destructive to the environment due to their stability and carcinogenic nature¹⁰.

2.2.2 Ring Formation

Ring formation is the process by which a paraffin or isoparaffin is brought into a five or six member ring, releasing one hydrogen molecule in the process. This reaction, which is a necessary precursor to the formation of aromatics, is quite a few orders of magnitude slower than aromatization and therefore is the limiting reaction in aromatic formation. Furthermore, the model predicts that a six-member ring forms more readily than a five-member ring, though not on a significant enough of a scale to favor one ring formation inherently over the other.

2.2.3 Isomerization

The isomerization reaction is one in which a section of non-branched or partly-branched hydrocarbon chain is shifted to another location on the base carbon chain, creating an isoparaffin or an isomer of the base ring compound. This reaction is split into four different reaction families based on the method by which the isomerizing chain is initially removed, then reattached to the base hydrocarbon chain (either from alpha, beta 1, beta 2, or gamma scission). This reaction, while not nearly as fast as the aromatization reaction, is still fairly fast compared to rate limiting reactions such as cracking. Furthermore, isomers are far more desirable than aromatics from an ecological standpoint, as isomers still produce high octane ratings while being better for biodegrading than highly stable aromatics.

2.2.4 Paraffin Cracking

Paraffin cracking is the process by which larger paraffins and i-paraffins are broken down into smaller fragments. While this reaction leads to yield loss (in the form of C1-C4 compounds, which do not stay in liquid form and are not accounted for by the reaction), cracking reactions are useful in that they transform heavy species (which are often over-represented by the catalytic model) and breaks them into smaller species, which replenish the smaller species that are lost due to cracking as well as to the rapid reactions of ring formation and aromatization. Like isomerization, paraffin cracking has four sub-families to address the various forms of scission that occur on the surface of the zeolite (alpha, beta 1, beta 2, and gamma scission). These reactions occur at a far slower pace than isomerization or ring formation, so yield loss from this method is minimal.

2.2.5 Ring Isomerization

This is the isomerization of a five-membered ring into a six-membered ring. The transformation of a cyclopentane to a cyclohexane is the necessary pathway for a five-membered ring to be transformed into an aromatic. This isomerization reaction is far slower than all other isomerization reactions, given that the system is already stable in a five-membered ring formation. This slows the formation of aromatics slightly, allowing for mid-sided paraffins and isoparaffins to still exist without being consumed completely into aromatics.

2.2.6 Side Chain Cracking

Side chain cracking differentiates itself from regular paraffin cracking in that in side chain cracking, the base substituent is a ring species that yields a paraffin or isoparaffin and a substituted ring product. This reaction is roughly the same rate as the other cracking species, and is a necessary reaction to decrease the size of the large aromatic products that are formed while also creating lighter paraffin products.

2.2.7 Dealkylation

Dealkylation is similar to side chain cracking, except that it also removes the substituent that was attached to the ring itself, producing far smaller aromatic products. However, since this carbon bond is held strongly by the stabilizing ring, the reaction rate of dealkylation is very low, with a fairly large activation energy. It therefore does not contribute greatly to the changes occurring in the model.

Chapter 3

EXPERIMENTAL SETUP

3.1 System Apparatus

To develop the tuned model, a computer of modest processing power (more than 1GHz and 4GB of RAM) was used, running Microsoft[®] Excel[®] 2007 with Visual[®] Basic capabilities. Furthermore, a Unix-like interpretation program called Cygwin[®] was used for the underlying C-code that did the true modeling of the process. The KME workbook employed is a graphical front-end which sent the changes in tuning parameters to Cygwin and the C-code, which then attempted to find the best possible solution with the constraints supplied. Typical experiment times ranged from a few minutes (when estimates were close to improved values) to a few hours (when the experiments ran out-of-bounds). These results were then reopened within the KME workbook for user analysis.

3.2 Experimental Data and Data Processing

Experimental data were retrieved from a pilot plant-level catalytic plug flow reactor¹¹ in the form of a PIANO summary. This summary reports the proportion of the summary brackets (determined by carbon number and hydrocarbon type) to the overall feed. These values are reported for both the reactant and product feeds to the plug flow reactor (PFR). The product PIANO summary is given in Table 4 in the Appendix.

Although the experimental data supplied are almost always given in a PIANO summary, KME requires the initial reactant concentrations to be given for every species in the model (Figure 3). These values, however, cannot be known: the reason PIANO summaries are used initially is that the concentrations for these individual species cannot be known due to the complex quantitative chemistry that would have to be used to isolate the compounds. Therefore, the initial assumption is that concentrations within each PIANO summary bracket are divided evenly amongst every isomer within that bracket. Using this assumption, the amount of available hydrogen (critical for the determination of the adsorption constants) is determined through stoichiometric calculations. The reactor output summaries (as supplied in Table 4) do not need to be similarly sorted amongst the isomers within the PIANO brackets, as KME summarizes the results into a PIANO summary already upon completion of the model.

	A				B	C	D
1	Mol/L	Reload	Save		Data1	Data2	Data3
16	species1(Mol/s)				8.54E-04	8.54E-04	8.54E-04
17	species23(Mol/s)				5.93E-06	5.93E-06	5.93E-06
18	species24(Mol/s)				6.10E-06	6.10E-06	6.10E-06
19	species33(Mol/s)				8.84E-05	8.84E-05	8.84E-05
20	species46(Mol/s)				9.69E-06	9.69E-06	9.69E-06
21	species47(Mol/s)				9.99E-06	9.99E-06	9.99E-06
22	species53(Mol/s)				6.30E-05	6.30E-05	6.30E-05
23	species54(Mol/s)				6.23E-05	6.23E-05	6.23E-05
24	species62(Mol/s)				9.94E-06	9.94E-06	9.94E-06
25	species67(Mol/s)				0	0	0
26	species73(Mol/s)				2.54E-04	2.54E-04	2.54E-04
27	species78(Mol/s)				6.49E-05	6.49E-05	6.49E-05
28	species83(Mol/s)				9.57E-05	9.57E-05	9.57E-05
29	species88(Mol/s)				6.06E-06	6.06E-06	6.06E-06
30	species91(Mol/s)				5.93E-06	5.93E-06	5.93E-06
31	species103(Mol/s)				8.84E-05	8.84E-05	8.84E-05
32	species112(Mol/s)				9.69E-06	9.69E-06	9.69E-06
33	species123(Mol/s)				6.30E-05	6.30E-05	6.30E-05

Figure 3: Species Input Sheet from KME

3.3 Initial Estimates

To determine the initial estimates for the tuning parameters ($\log A$ and E_0 , as the α parameter is initially assumed to be 0), a literature search was done on older papers employing Arrhenius assumption for a simplified reaction constant^{12,13,14}. In addition to this, many $\log A$ and E_0 initial estimates were supplied from a previous, simplified catalytic reforming model developed by the Klein Research Group. Using these sources, the list of initial parameters used (Table 2) were used in the tuning method, as outlined in Section 3.4.

Table 2: Summary of Initial Tuning Estimates

Reaction Group	logA	E₀ [kCal/mol]
Aromatics	18	30
Paraffin Cyclization	10	40
Isomerization	5	35
Cracking	10	30
Remaining Reaction Families	10	30

3.4 Tuning Method

In order to adjust the initial tuning estimates within reasonable ranges so that the model can more closely predict the experimental results, the tuning system KME has for turning on and off tuning (holding some parameters constant while others are varied) was used. Once a valid range was set for the tuning parameters being changed (with α parameters being required to be within -0.5 to .5) and they were turned "on" (1) instead of "off" (0), KME then saved the changes and loaded the model into the underlying C-code (Figure 4). Once the model was loaded into the code, KME would begin running Monte Carlo simulations based on simplified graph theory to lower the difference between the experimental and model-calculated results.

	A	B	C	D	E
1	OPT	Name	Value	LB	UB
2	1	IgA1	18.954522	18	23
3	0	E1	30.142337	29	31
4	1	dS1	-0.357986	-0.5	-0.3
5	0	dH1	0	0	0
6	0	IgA2	2.890764	1.5	4.5
7	0	E2	45	32	38
8	0	dS2	-0.302519	-0.6	0
9	0	dH2	0	0	0
10	0	IgA3	11.079611	10	15
11	0	E3	38.477204	35	40
12	0	dS3	0.048988	-0.1	0.25
13	0	dH3	0	0	0
14	0	IgA4	14.766558	11	17
15	0	E4	38.477204	34	42
16	0	dS4	-0.017452	-0.1	0.25
17	0	dH4	0	0	0
18	0	IgA5	3.241292	3	7
19	0	E5	30	27	35
20	0	dS5	0.282975	0	0.4
21	0	dH5	0	0	0
22	1	IgA6	2.922516	2	6
23	0	E6	31.892974	28	34
24	1	dS6	0.156777	-0.1	0.5
25	0	dH6	0	0	0
26	0	IgA7	3.851884	3	7
27	0	E7	30	27	35
28	0	dS7	0.26842	0	0.5
29	0	dH7	0	0	0
30	1	IgA8	2.582285	2	6
31	0	E8	33.456637	28	34
32	1	dS8	0.470747	-0.1	0.5

Figure 4: KME Tuning Sheet, with Some Reaction Parameters Activated

Once a particular tuning experiment was completed (or canceled by the user due to the system leaving the pre-set bounds), an overall parity plot was then generated. This parity plot would visually represent how accurate the model is, as well as highlight which observed products were most clearly misrepresenting the experimental data. The modeler would then change the pre-set bounds or change which reaction families were being tuned to further improve the accuracy of the

model. Figure 13 in the Appendix shows one such parity plot where many of the model-predicted results varied significantly from the experimental results.

3.5 Individual Reactions

While the initially defined model (with 14 large reaction families) was being tuned, it became apparent that certain species were being chronically misrepresented by the model (Figure 13 in the Appendix). Most notably, the production of A7 (toluene) was significantly underrepresented by the model. This was unexpected, as the reaction family that produced most of the toluene has the highest reaction rate of all of the other reaction families. Upon comparing the activation energy calculated by the model to the literature¹⁵, it was discovered that the reaction family was drastically overestimating the activation energy of the dehydrogenation reaction that produced toluene (54 kcal/mol instead of roughly 30 kcal/mol). This difference is likely due to the reaction family attempting to better approximate the other reactions in the dehydrogenation reaction family, which left toluene to be inaccurate. To rectify this, the single reaction that generates toluene from methylcyclohexane was removed from the dehydrogenation reaction family and put into a reaction family of its own (an "individual reaction"). In doing so, the model was then able to far better predict both toluene and also all other aromatic products from the reactions.

3.6 Carbon Length Dependence

In developing the model, it became clear that certain reactions (in particular, cracking) were resulting in the model over-representing the heavier components in the system. This is due primarily to the fact that, despite the need for cracking reactions to produce the lower weight species, the high rate of cracking needed by the model

was predicting a far higher yield loss (cracking reactions resulting in C1-C4 compounds) than what was shown by the data. The cracking of the larger species was proceeding slower than the data predicted, while the cracking of the smaller species were proceeding faster than the data predicted. Therefore, the implementation of carbon-dependence parameter was necessary to balance the cracking reactions:

$$C_{\text{fix}} = \left(\frac{\text{Carbon \#}}{5} \right)^{\beta} \quad (9)$$

where β is a new tuning parameter used specifically to account for the degree that the size of the molecule being cracked effects the reaction rate.

fairly accurately models the catalytic reforming reaction. The outliers, and their relative sources, are addressed in the following species parity plots.

4.2 Aromatic Analysis

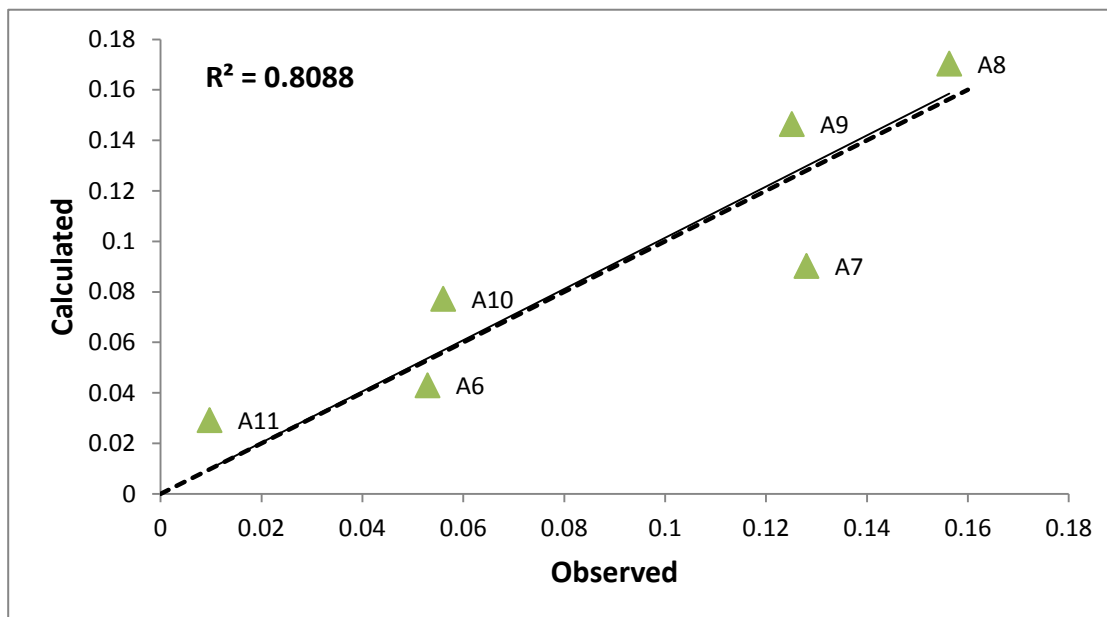


Figure 6: Aromatic Parity of the Catalytic Reforming Model

As indicated in Figure 6, the parity for aromatic formation between experimental and model is nearly exact. The inclusion of toluene's own reaction family removed it from being an outlier (as it is in Figure 13) and changes the material to being slightly overrepresented rather than grossly underrepresented. Furthermore, since the production of aromatics is by far the most important reaction to occur in the catalytic reformer (for both octane level and environmental risks), the strong parity present in the aromatics model indicates that the overall model is accurate.

4.3 Isoparaffin Analysis

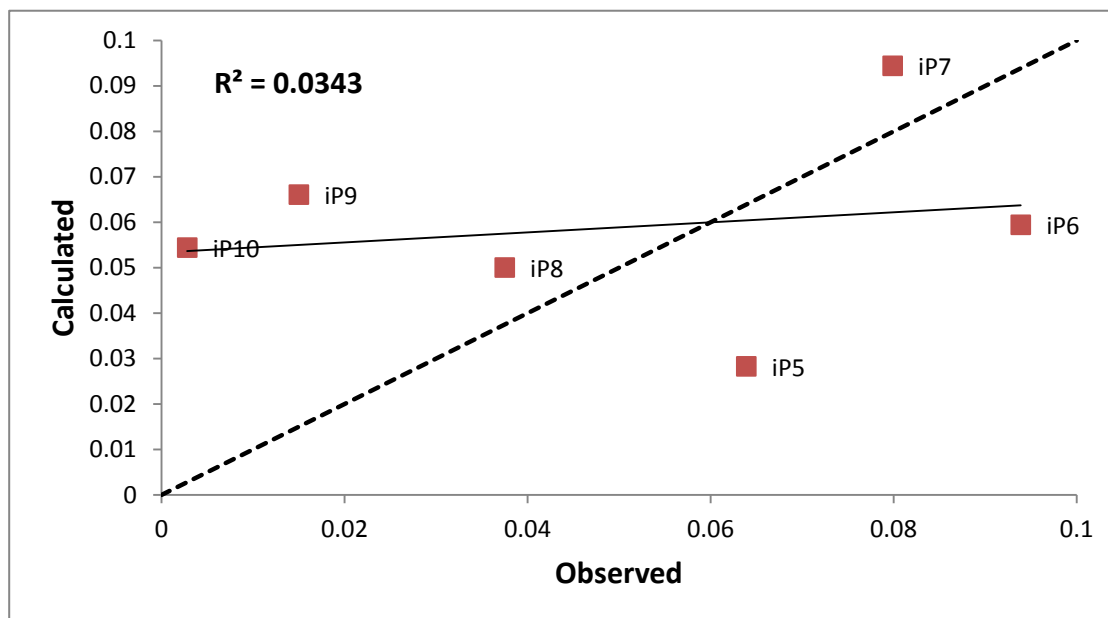


Figure 7: Isoparaffin Parity of the Catalytic Reforming Model

The parity presented in Figure 7 for isoparaffins is far less accurate than the one presented for aromatics. Here, the heavier isoparaffins are grossly overrepresented, while the smaller isoparaffins are underrepresented. It becomes clear that the system, in addition to lowering how quickly larger paraffins are isomerized into isoparaffins, must also raise the rate at which the larger i-paraffins are cracked into smaller (C5-C8) i-paraffins. In addition to raising the i-paraffin concentration in this manner, the increased cracking would address the inaccuracies presented in the paraffin parity plot, represented in Figure 8 while maintaining a strong aromatic parity.

4.4 Paraffin Analysis

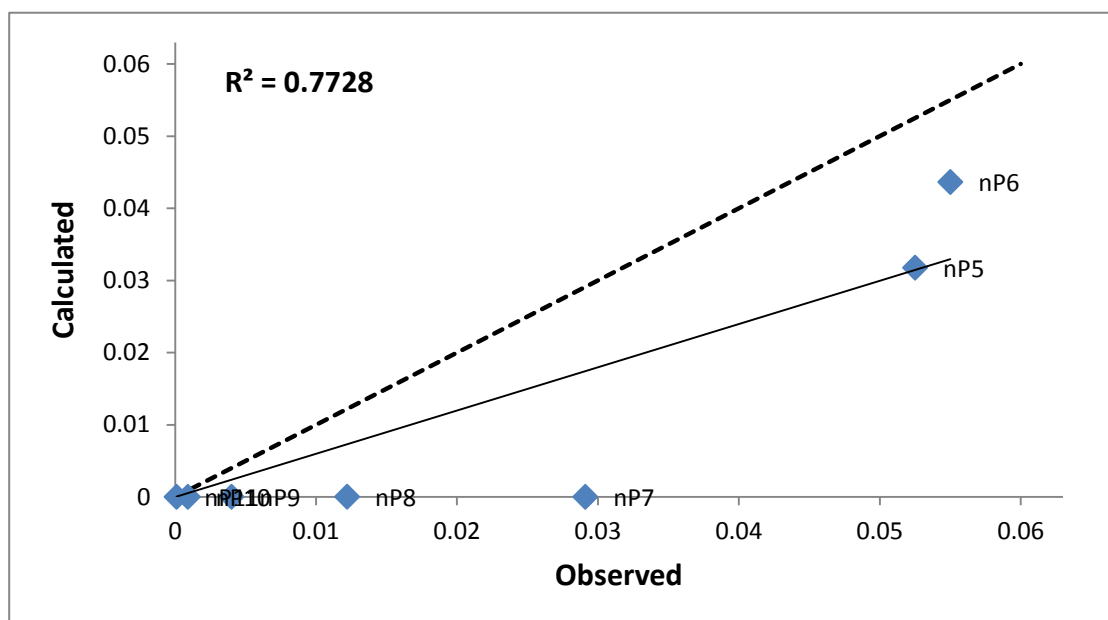


Figure 8: Paraffin Parity of the Catalytic Reforming Model

The paraffin parity presented in Figure 8, due to having far lower concentrations overall when compared to the isoparaffin and aromatic content, does not have significant deviations from parity. The only aspect of the paraffin model that is poorly matched to experimental data is that of nP7 (heptane). According to the model, this material is completely used up in the reaction, primarily in the ring formation to methylcyclohexane, which then quickly converts to toluene (which was used to improve the aromatic parity). Therefore, slower isomerization and higher cracking would greatly benefit this one outlier, as well as slower ring formation in the model.

4.5 Naphthene Analysis

Naphthene, being present in extremely small concentrations by the completion of the reaction (due mainly to being used completely in the creation of aromatics), is clustered very close to 0 in the overall parity plot in Figure 5. Due to its minuscule concentration in the feed, the amount present for these species is far less than the error present for the experimental data itself. Therefore, a parity plot of this group does not reflect any value towards the accuracy of the model itself, and therefore cannot be analyzed.

Chapter 5

FUTURE WORK

5.1 Temperature Dependence

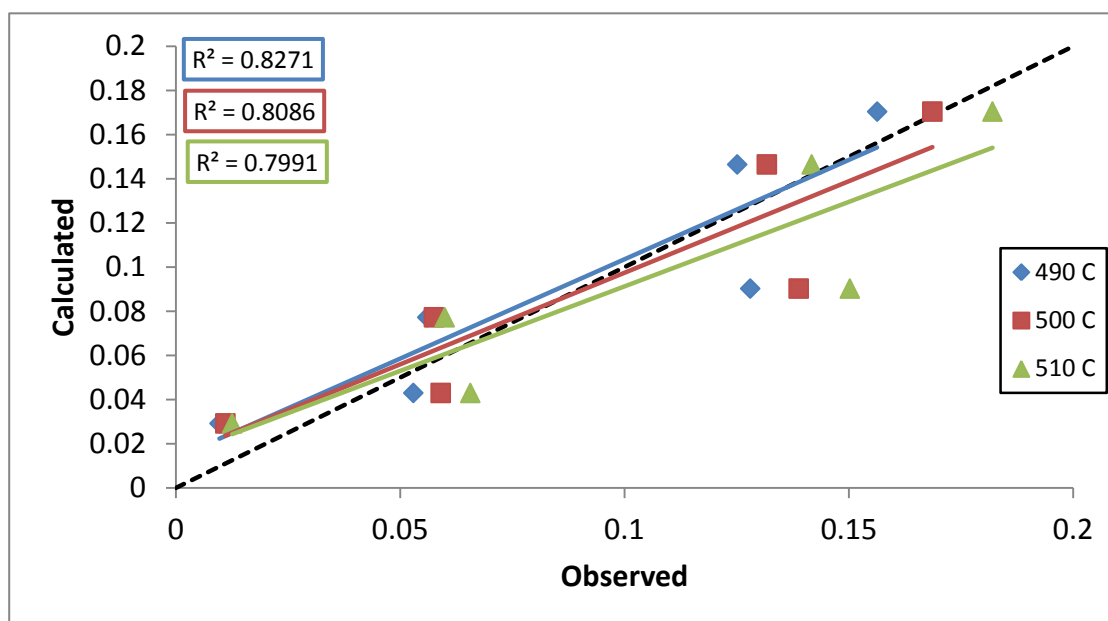


Figure 9: Aromatic Parity Plots for Varying Temperatures

The reforming model encounters difficulty when there is a change in the temperature profile, as indicated by Figure 9. The variance in temperature, although slight, causes the aromatic modeling parameters (which has been determined

previously to be the most accurate) to deviate strongly. Furthermore, the deviations become more difficult to predict the further the temperature deviates from the initial fitting data (as indicated by the rapidly decreasing R^2 value). Therefore, further consideration must be given to the development of the model's temperature dependence.

5.2 Semi-Regenerative Reforming

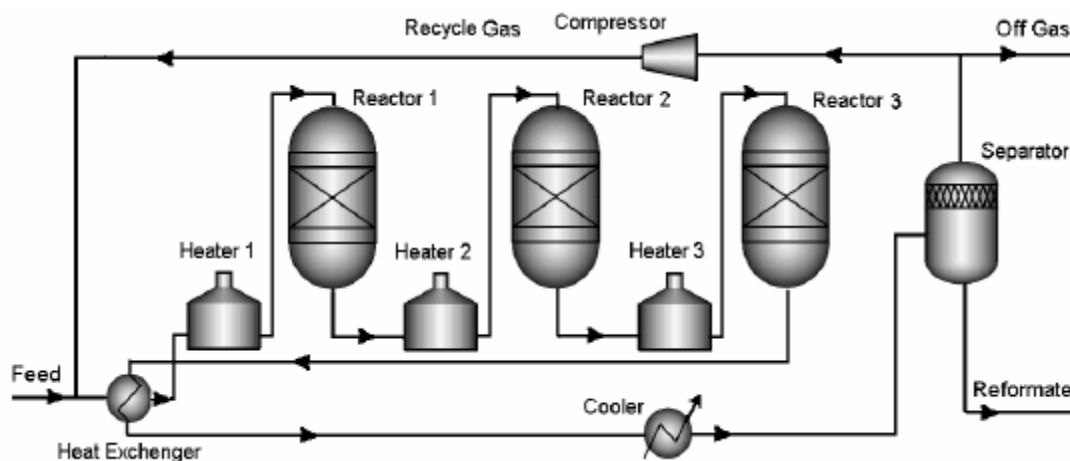


Figure 10: Simplified Flowsheet of Semi-Regenerative Reforming

Upon verifying the accuracy of the reforming model on pilot-plant data, the first industrial-scale process that the model would be applied on would be a semi-regenerative reforming process. This process, which is outlined in Figure 10, is motivated by the magnitude of the temperature profile experienced by the reactors and the deactivation of the catalyst. The aromatization reactions, the fastest set of reactions in the model, are highly endothermic: therefore, the beginning of the

catalytic reformer experiences a significant temperature drop. This necessitates that the process be reheated to maintain a high reaction rate, resulting in three or four plug flow reactors. Furthermore, the deactivation of the catalyst due to carbon soot filling active sites (or “coking”) requires that the process be shut down for maintenance clean the catalyst (the “semi-regenerative” aspect of the process). Applying the reforming model to the semi-regenerative reforming process, in addition to accounting for the coking process, would finalize the model and have it prepared for refinery modeling.

5.3 Overall Refinery Model

The reforming model, once completed, would give an accurate representation of the catalytic reforming process in a refinery. Due to the modular design of the models created by the Kinetic Modeling Editor, though, this finalized model does not have to be considered in and of itself. Rather, the model would be used in conjunction with other models developed by the Klein Research Group (hydrotreating, pyrolysis, etc.) to give an overall representation of the operations within a refinery, from the overall initial feedstock to all finalized products. Refineries could then be designed and sized based off of one unified model of a refinery and the “Universal Oil” feedstock.

Chapter 6

CONCLUSIONS

The development of the catalytic reforming process using pathways modeling methods requires strong modeling tools as well as knowledge of the reaction kinetics of the major species. Using the tools in the Kinetic Modeling Toolkit (KMT) and literature data, a modular yet complex model was developed to account for the difficulties presented by catalytic reforming. Using an initial analysis of five types of reactions (aromatization, ring formation, isomerization, cracking and dealkylation), the reactions were organized into 14 multi-component reaction families and one individual reaction (toluene) to account for the difference of toluene to all other aromatic compounds. In using these 15 different reaction groups, in addition to the inclusion of a carbon length dependence, the model was able to predict the production of aromatic products accurately while giving insight onto how to improve the accuracy of the other aspects of the model.

In addition, further development of the current reforming model in the areas of temperature dependence and coking analysis could greatly increase the accuracy of the model. These changes have the potential to create a highly complex (greater than 500 key reactions) yet quick to solve (within 5 seconds) model on catalytic reforming. Applying this model to other modules developed by Klein Research Group allows for the modeling of an entire refinery regardless of feed concentrations.

REFERENCES

1. Marshall, E. L., and Owen, K., eds. (1995). *Critical Reports on Applied Chemistry*, Vol. 34: *Motor Gasoline*. Cambridge, U.K.: Royal Society of Chemistry.
2. Klein, M. T., Hou, G., Bertolacini, R. J., Broadbelt, L. J., & Kumar, A. (2006). *Molecular modeling in heavy hydrocarbon conversions*. (pp. 2-6). Boca Raton: Taylor & Francis Group.
3. Joshi, P., Klein, M. T., Huebner, A., & Leyerle, R. (1999). *Automated modeling of catalytic reforming at the reaction pathways level*. (2nd ed., pp. 169-193). Boca Raton: Taylor & Francis.
4. Ramage, M., Graziani, K., & Krambeck, F. J. (1980). Development of mobil's kinetic reforming model. *Chemical Engineering Science*, 35, 42-48.
5. Kmak, W. S., & Stuckey, Jr., A. N. (1973, March). In W. S. Kmak (Chair). *Powerforming process studies with a kinetic simulation model*. Aiche national meeting, New Orleans, Louisiana.
6. Roberts, G. (2009). *Chemical reactions and chemical reactors*. (1st ed., pp. 305-378). Danvers, MA: Wiley.
7. Hou, Zhen (2011) Software tools for molecule-based kinetic modeling of complex systems. *Rutgers State University of New Jersey, Chemical Engineering Department*.
8. Mochida, I., & Yoneda, Y. (1967). Linear free energy relationships in heterogeneous catalysis: III. Temperature Effects in Dealkylation of Alkylbenzenes on the Cracking Catalysts. *Journal of Catalysis*, 8, 223-230.
9. M. G. Evans and M. Polanyi *Trans. Faraday Soc.*, 1938,34, 11-24
10. US Environmental Protection Agency. (1994, August). *Chemical summary for toluene*. Retrieved from http://www.epa.gov/chemfact/s_toluen.txt
11. Ancheyta-Juarez, J., & Villafuerte-Macias, E. (2000). Kinetic modeling of naphtha catalytic reforming reactions. *Energy & Fuels*, 14, 1032-1037.

12. Franklin, J. L., & Nicholson, D. E. (1955). Kinetic study of the decomposition of hydrocarbons by silica-alumina catalysts. *Decomposition of Hydrocarbons by Silica-Alumina Catalysts*, 60, 59-62.
13. Mochida, I., & Yoneda, Y. (1967). Linear free energy relationships in heterogeneous catalysis: I. Dealkylation of Alkylbenzenes on Cracking Catalysts. *Journal of Catalysis*, 7, 386-392.
14. Mochida, I., & Yoneda, Y. (1967). Linear free energy relationships in heterogeneous catalysis: II. Dealkylation and Isomerization Reactions on Various Solid Acid Catalysts. *Journal of Catalysis*, 7, 393-396.
15. Sinfelt, J. H., Hurwitz, H., & Shulman, R. A. (1960). Kinetics of methylcyclohexane dehydrogenation over pt-al₂o₃. *Industrial Engineering Chemistry*, 64, 1559-1562.

Appendix

ADDITIONAL FIGURES AND TABLES

Table 3: Catalytic Reforming Model Output Totals from INGen

Reaction Family	# of Reactions	Reaction Family	# of Reactions
Aromatization	22	Isomerization: Ring	45
Cyclization, C5	31	Cracking: Path A	9
Cyclization, C6	21	Cracking: Path B1	105
Isomerization: Path A	38	Cracking: Path B2	20
Isomerization: Path B1	32	Cracking: Path C	60
Isomerization: Path B2	44	Cracking: Side Chain	36
Isomerization: Path C	100	Dealkylation	19
		Total	582

Table 4: PIANO Summary of Effluent From Catalytic Reformer

PIANO Index	T = 763.15 K	T = 773.15 K	T = 783.15 K
Paraffin 5	0.0525	0.0496	0.0485
Paraffin 6	0.055	0.0521	0.044
Paraffin 7	0.0291	0.0244	0.0197
Paraffin 8	0.0122	0.0091	0.0063
Paraffin 9	0.004	0.0028	0.0018
Paraffin 10	0.0009	0	0
Paraffin 11	0.0001	0.0001	0
Paraffin 12	0	0	0
Isoparaffin 5	0.0639	0.0618	0.0553
Isoparaffin 6	0.0939	0.0948	0.0983
Isoparaffin 7	0.0799	0.0727	0.0607
Isoparaffin 8	0.0375	0.0274	0.0201
Isoparaffin 9	0.015	0.0124	0.0067
Isoparaffin 10	0.0028	0.0017	0.0085
Isoparaffin 11	0	0	0
Naphthene 5	0	0	0

Naphthene 6	0.0136	0.0124	0.0116
Naphthene 7	0.0033	0.0031	0.0027
Naphthene 8	0.0063	0.0066	0.0038
Naphthene 9	0.0001	0.0002	0.0001
Naphthene 10	0	0	0
Naphthene 11	0	0	0
Naphthene 12	0	0	0
Aromatic 6	0.0529	0.059	0.0656
Aromatic 7	0.128	0.1388	0.1502
Aromatic 8	0.1563	0.1686	0.182
Aromatic 9	0.1251	0.1317	0.1417
Aromatic 10	0.056	0.0575	0.0599
Aromatic 11	0.0097	0.011	0.0125
Aromatic 12	0	0	0

Table 5: Raw Tuned Parameters of Reforming Model

Reaction Family	logA	E₀	α
Aromatization	18.954522	30.142337	-0.357986
Cyclization, C5	2.890764	45	-0.302519
Cyclization, C6	11.079611	38.477204	0.048988
Isomerization: Path A	14.766558	38.477204	-0.017452
Isomerization: Path B1	3.241292	30	0.282975
Isomerization: Path B2	2.922516	31.892974	0.156777
Isomerization: Path C	3.851884	30	0.26842
Isomerization: Ring	2.582285	33.456637	0.470747
Cracking: Path A	3.625395	30	0.351811
Cracking: Path B1	2.324651	30	0.05159
Cracking: Path B2	3.900964	30	0.193515
Cracking: Path C	10.967552	31.904885	0.48281
Cracking: Side Chain	5.709591	30	0
Dealkylation	2.692422	31.141262	0
Toluene Reaction	24.845746	29.30221	0

		<div style="display: flex; justify-content: space-between; align-items: center;"> BUILD MODEL LOAD RTK SAVE RTK </div>			
C:KME5.0\Models\Refined_Reforming\lrxn.eqn		lgA	E	ΔS	ΔH
REACTIONS		(1/sec·atm ^(v-1))	(kcal/mol)	(kcal/mol·K)	(kcal/mol)
1	RF1 <=> RF1	22.778529	30.142337	-0.486004	0
2	RF2 <=> RF2	2.890764	45	-0.302519	0
3	RF3 <=> RF3	11.24298	38.477204	0	0
4	RF4 <=> RF4	13.937131	38.477204	0	0
5	RF5 <=> RF5	3.241292	30	0.282975	0
6	RF6 <=> RF6	2.136017	31.892974	0.213269	0
7	RF7 <=> RF7	3.851884	30	0.26842	0
8	RF8 <=> RF8	3.796415	33.456637	0.047874	0
9	RF9 <=> RF9	3.625395	30	0.351811	0
10	RF10 <=> RF10	2.413678	30	0.336756	0
11	RF11 <=> RF11	3.900964	30	0.193515	0
12	RF12 <=> RF12	6.620923	31.904885	0.433134	0
13	RF13 <=> RF13	5.709591	30	0	0
14	RF14 <=> RF14	2.692422	31.141262	0	0
15	species1 + [L1] <=> species1[L1]	0	0	0	0
16	species23 + [L1] <=> species23[L1]	0	0	0	0
17	species24 + [L1] <=> species24[L1]	0	0	0	0
18	species33 + [L1] <=> species33[L1]	0	0	0	0
19	species46 + [L1] <=> species46[L1]	0	0	0	0

Figure 11: Raw Reaction Equations of Catalytic Reforming Model in KME

D174		$K_{eq}[171]=0.182+(1.93^{*}gproplis[species136][SAromRingNum]+0.187^{*}(gproplis[species136][STotalCarbonNum]-gproplis[species136][SAromCNum]))/(8.314^{*}TEMP);$			
B	C	D	E	F	G
14	RF14 <=> RF14	rxn[13]=0;			
15	species1 + [L1] <=> species1[L1]	$K_{eq}[14]=0.182+(1.93^{*}gproplis[species1][SAromRingNum]+0.187^{*}(gproplis[species1][STotalCarbonNum]-gproplis[species1][SAromCNum]))/(8.314^{*}TEMP);$			
16	species23 + [L1] <=> species23[L1]	$K_{eq}[15]=0.182+(1.93^{*}gproplis[species23][SAromRingNum]+0.187^{*}(gproplis[species23][STotalCarbonNum]-gproplis[species23][SAromCNum]))/(8.314^{*}TEMP);$			
17	species24 + [L1] <=> species24[L1]	$K_{eq}[16]=0.182+(1.93^{*}gproplis[species24][SAromRingNum]+0.187^{*}(gproplis[species24][STotalCarbonNum]-gproplis[species24][SAromCNum]))/(8.314^{*}TEMP);$			
18	species33 + [L1] <=> species33[L1]	$K_{eq}[17]=0.182+(1.93^{*}gproplis[species33][SAromRingNum]+0.187^{*}(gproplis[species33][STotalCarbonNum]-gproplis[species33][SAromCNum]))/(8.314^{*}TEMP);$			
19	species46 + [L1] <=> species46[L1]	$K_{eq}[18]=0.182+(1.93^{*}gproplis[species46][SAromRingNum]+0.187^{*}(gproplis[species46][STotalCarbonNum]-gproplis[species46][SAromCNum]))/(8.314^{*}TEMP);$			
20	species47 + [L1] <=> species47[L1]	$K_{eq}[19]=0.182+(1.93^{*}gproplis[species47][SAromRingNum]+0.187^{*}(gproplis[species47][STotalCarbonNum]-gproplis[species47][SAromCNum]))/(8.314^{*}TEMP);$			
21	species53 + [L1] <=> species53[L1]	$K_{eq}[20]=0.182+(1.93^{*}gproplis[species53][SAromRingNum]+0.187^{*}(gproplis[species53][STotalCarbonNum]-gproplis[species53][SAromCNum]))/(8.314^{*}TEMP);$			
22	species54 + [L1] <=> species54[L1]	$K_{eq}[21]=0.182+(1.93^{*}gproplis[species54][SAromRingNum]+0.187^{*}(gproplis[species54][STotalCarbonNum]-gproplis[species54][SAromCNum]))/(8.314^{*}TEMP);$			
23	species62 + [L1] <=> species62[L1]	$K_{eq}[22]=0.182+(1.93^{*}gproplis[species62][SAromRingNum]+0.187^{*}(gproplis[species62][STotalCarbonNum]-gproplis[species62][SAromCNum]))/(8.314^{*}TEMP);$			
24	species67 + [L1] <=> species67[L1]	$K_{eq}[23]=0.182+(1.93^{*}gproplis[species67][SAromRingNum]+0.187^{*}(gproplis[species67][STotalCarbonNum]-gproplis[species67][SAromCNum]))/(8.314^{*}TEMP);$			
25	species73 + [L1] <=> species73[L1]	$K_{eq}[24]=0.182+(1.93^{*}gproplis[species73][SAromRingNum]+0.187^{*}(gproplis[species73][STotalCarbonNum]-gproplis[species73][SAromCNum]))/(8.314^{*}TEMP);$			
26	species78 + [L1] <=> species78[L1]	$K_{eq}[25]=0.182+(1.93^{*}gproplis[species78][SAromRingNum]+0.187^{*}(gproplis[species78][STotalCarbonNum]-gproplis[species78][SAromCNum]))/(8.314^{*}TEMP);$			
27	species83 + [L1] <=> species83[L1]	$K_{eq}[26]=0.182+(1.93^{*}gproplis[species83][SAromRingNum]+0.187^{*}(gproplis[species83][STotalCarbonNum]-gproplis[species83][SAromCNum]))/(8.314^{*}TEMP);$			
28	species88 + [L1] <=> species88[L1]	$K_{eq}[27]=0.182+(1.93^{*}gproplis[species88][SAromRingNum]+0.187^{*}(gproplis[species88][STotalCarbonNum]-gproplis[species88][SAromCNum]))/(8.314^{*}TEMP);$			
29	species91 + [L1] <=> species91[L1]	$K_{eq}[28]=0.182+(1.93^{*}gproplis[species91][SAromRingNum]+0.187^{*}(gproplis[species91][STotalCarbonNum]-gproplis[species91][SAromCNum]))/(8.314^{*}TEMP);$			
30	species103 + [L1] <=> species103[L1]	$K_{eq}[29]=0.182+(1.93^{*}gproplis[species103][SAromRingNum]+0.187^{*}(gproplis[species103][STotalCarbonNum]-gproplis[species103][SAromCNum]))/(8.314^{*}TEMP);$			
31	species112 + [L1] <=> species112[L1]	$K_{eq}[30]=0.182+(1.93^{*}gproplis[species112][SAromRingNum]+0.187^{*}(gproplis[species112][STotalCarbonNum]-gproplis[species112][SAromCNum]))/(8.314^{*}TEMP);$			
32	species123 + [L1] <=> species123[L1]	$K_{eq}[31]=0.182+(1.93^{*}gproplis[species123][SAromRingNum]+0.187^{*}(gproplis[species123][STotalCarbonNum]-gproplis[species123][SAromCNum]))/(8.314^{*}TEMP);$			
33	species140 + [L1] <=> species140[L1]	$K_{eq}[32]=0.182+(1.93^{*}gproplis[species140][SAromRingNum]+0.187^{*}(gproplis[species140][STotalCarbonNum]-gproplis[species140][SAromCNum]))/(8.314^{*}TEMP);$			
34	species145 + [L1] <=> species145[L1]	$K_{eq}[33]=0.182+(1.93^{*}gproplis[species145][SAromRingNum]+0.187^{*}(gproplis[species145][STotalCarbonNum]-gproplis[species145][SAromCNum]))/(8.314^{*}TEMP);$			
35	species146 + [L1] <=> species146[L1]	$K_{eq}[34]=0.182+(1.93^{*}gproplis[species146][SAromRingNum]+0.187^{*}(gproplis[species146][STotalCarbonNum]-gproplis[species146][SAromCNum]))/(8.314^{*}TEMP);$			
36	species165 + [L1] <=> species165[L1]	$K_{eq}[35]=0.182+(1.93^{*}gproplis[species165][SAromRingNum]+0.187^{*}(gproplis[species165][STotalCarbonNum]-gproplis[species165][SAromCNum]))/(8.314^{*}TEMP);$			
37	species3 + [L1] <=> species3[L1]	$K_{eq}[36]=0.182+(1.93^{*}gproplis[species3][SAromRingNum]+0.187^{*}(gproplis[species3][STotalCarbonNum]-gproplis[species3][SAromCNum]))/(8.314^{*}TEMP);$			
38	species93 + [L1] <=> species93[L1]	$K_{eq}[37]=0.182+(1.93^{*}gproplis[species93][SAromRingNum]+0.187^{*}(gproplis[species93][STotalCarbonNum]-gproplis[species93][SAromCNum]))/(8.314^{*}TEMP);$			
39	species94 + [L1] <=> species94[L1]	$K_{eq}[38]=0.182+(1.93^{*}gproplis[species94][SAromRingNum]+0.187^{*}(gproplis[species94][STotalCarbonNum]-gproplis[species94][SAromCNum]))/(8.314^{*}TEMP);$			
40	species114 + [L1] <=> species114[L1]	$K_{eq}[39]=0.182+(1.93^{*}gproplis[species114][SAromRingNum]+0.187^{*}(gproplis[species114][STotalCarbonNum]-gproplis[species114][SAromCNum]))/(8.314^{*}TEMP);$			

Figure 12: Reaction Constants of Catalytic Reforming Model in KME

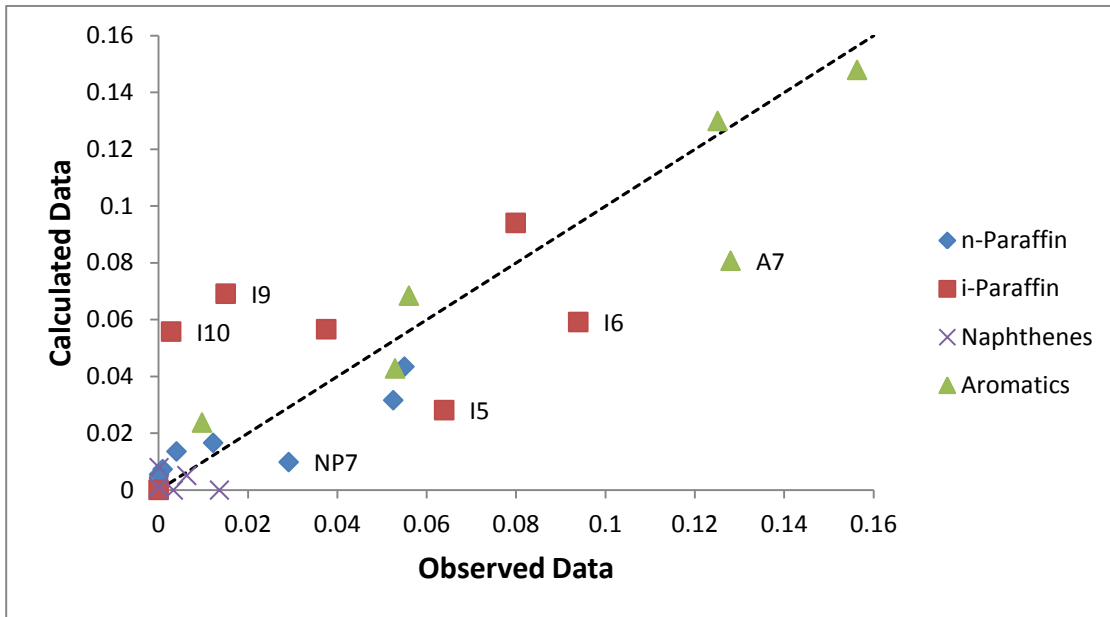


Figure 13: Overall Parity Plot, Prior to Inclusion of A7 Individual Reaction